PID Controller Design for "in vitro" Exposure System at Mobile Phone Frequencies

R. Iervolino*, R. Massa**

**Dipartimento di Informatica e Sistemistica, University of Naples, Naples, Italy (email: rafierv@unina.it)*
***Dipartimento di Scienze Fisiche, University of Naples, Naples, Italy (e-mail: rita.massa@unina.it)*

Abstract: In the recent years, the analysis of the possible dangerous biological effects of electromagnetic fields at mobile phone frequencies has become of relevant interest for the scientific community. The availability of a controlled exposure system may help in performing meaningful experiments. To this aim, a suitable PID control is designed starting from a mathematical model of the exposure system. Both the structure and the parameters of the proposed model are derived directly from the experimental results. The effectiveness of the controller is also demonstrated via experimental evaluations.

Keywords: PID control, model-based control, mathematical model, electromagnetic field problems, power control, dosimetry, exposure setup, UMTS

1. INTRODUCTION

Motivated by the growing use of modern telecommunications technology, a big research effort has been spent in the last years to investigate about the possibility that the electromagnetic fields could be responsible for particular health damages. To this end a huge number of experiments, both *in vivo* and *in vitro*, were carried out aiming at the evaluation of possible biological effects of electromagnetic fields at frequencies used by mobile phones (800 MHz – 3000 MHz). The obtained results were however inconclusive or conflicting and often difficult to replicate mostly due to the inadequate knowledge and reproducibility of the exposure conditions, in other words to inaccurate dosimetry control, see Paffi et al. (2010). Deep discussions on quality assurance of exposure systems were carried out as pointed out by a number of workshops and publications yielded by the scientific community; the recommended minimum requirements for exposure systems, in order to obtain reproducible and scientifically valuable results, are synthesized in Kuster and Schönborn (2000).

In this context, the appropriate control of the SAR (*Specific Absorption Rate*: the absorbed power per unit mass of the exposed sample [W/kg]) during the exposure plays a fundamental role. The knowledge of the SAR and its distribution into the sample as well as its control during the exposure are crucial in order to avoid misleading results due to the well-known thermal effects that can occur whit high SAR levels. Depending on the objective of the research about the evaluation of "non-thermal effects" induced by electromagnetic field, the protocol of the experiment could require, at a desired SAR level, a continuous or intermittent (i.e. 5 min on - 10 min off) or pulsed exposure, in order to mimic real life situation in which population is exposed. The treatment duration can be long (i.e. 18h, 24 h) or short (few minutes, for example for kinetic studies). Another feature of these studies concerns the experimental dosimetry carried out in order to validate the results of the electromagnetic field distribution obtained by means of commercial codes. To this end the thermal increase of the sample exposed to very high SAR levels is typically measured during the first about 30s of exposures in order to prevent artifacts due to thermal diffusion.

This implies that, especially for the short time exposure experiments, a sufficiently fast achievement of the desired input power source that feeds the exposure applicator has to be guaranteed. According to the assumed protocol, all the specific experimental requirements may be attained if an appropriate controller is designed and integrated in the exposure system.

In this paper the design problem of a suitable PID controller for *in vitro* exposure system is considered. In particular, the settings of the proposed PID controller are based upon the mathematical model of the exposure system and are chosen so that the controlled response adhere to given specifications (see Åström and Hagglund (1995)). Some experimental results are also reported to demonstrate the effectiveness of the proposed control scheme.

Remarkably, the experimental set-up described in this paper has been widely employed in experiments carried out at the Electromagnetic Safety Pole within the framework of the Regional Centre on Information and Communication Technologies of Campania Region (CerICT), aimed at the detection of carcinogenic effects in cell cultures exposed to UMTS (Universal Mobile Telecommunications System) signals (i.e. 1.95Hz) in several recent research projects. The aim of the projects and the details of the components of the

exposure system are widely described in (Calabrese et al. (2004) and Calabrese et al. (2006)).

The paper is organised as follows. In Section 2 the considered exposure system is briefly introduced. In Section 3 the mathematical models of the various components and of the global system are presented. In Section 4 the PID control law design is illustrated. Section 5 demonstrates with some experimental results the effectiveness of the proposed controller. Finally, Section 6 summarizes our study.

2. THE EXPERIMENTAL SET-UP

In Fig. 1 a photo of the exposure system is reported. The UMTS signal, generated by a signal generator (Agilent E4432B ESG-D series), is amplified (Microwave Amplifiers LtdAM38A-092S-40-43) and fed through a bidirectional power sensor (NRT-Z43 Rohde&Schwarz) and a coaxial cable into a thermostated waveguide (WR-430, 109.2mm×54.6mm) terminated with a short circuit plate. The applicator was housed in a commercial incubator in order to ensure environmentally controlled exposure as well as cell culture conditions (air with 5% CO_2, temperature 37±0.5°C, humidity 95%). With the aim of avoiding a long permanence of power sensors into this environment, a coaxial cable was needed to connect the applicator to the rest of the feeding circuit.

Four Petri dishes (Falcon, 3001T, 35mm diameter), filled with 3ml cell culture, are placed in a plastic dish holder (see Fig. 2) and positioned inside the waveguide, allowing simultaneous irradiation at two different SAR levels. The two internal (central) samples are exposed at a SAR that is four times higher than that of the external samples (upper and lower). The bidirectional power sensor allows the measurements of the *incident* power (P_i), i.e. coming from the amplifier, and the *reflected* power (P_r), i.e. coming from the applicator, and, thus, the evaluation of the absorbed power ($P_a = P_i - P_r$) and the average SAR level. Both the signal generator and power sensor are connected to a computer for the continuous control of the power level. In all the experiments a tight control of the SAR is required during the exposure and the achievement of the desired value is obtained starting from an extremely low level (-40 dBm). In this way undesired SAR values that could induce an increase of temperature and, as consequence, a thermal effect on the cell culture are avoided. Power peak values can actually occur due to the initial instability or thermal drift of the source and/or the amplifier.

For the sake of completeness, it must be noted that the same exposure system is also used for local SAR measurements, necessary for the validation of numerical simulations that allow the knowledge of SAR distribution, and thus of power uniformity, into the sample. The local SAR values are calculated from the temperature, measured with a fiber optic thermometer (FISO Technologies, FOT-M/2m) opportunely inserted into the sample. In particular, the initial temperature derivative is known to be proportional to the SAR in the first few seconds of high power level exposure. According to Moros and Pickard (1999), the time window (t_m), over which temperature variation associated with SAR is measured, satisfies the inequality $t_m \leq \delta^2/(\pi^2 D)$, where δ [m] is the half-width at half-maximum of the SAR distribution and D [m^2/s] is the thermal diffusivity. Being t_m of the order of 30 – 60s, the possibility of achieving the desired SAR level in a sufficiently shorter time interval, and of ensuring the "stability" of its steady-state value by means of the PID control is really attractive.

Thanks to previous research works, see Calabrese et al. (2006), the conditions that influence the sample exposure (such as the support material, dimensions and distance from the end of the waveguide, etc.) were already known. These parameters were preliminarily chosen to guarantee the sample absorbed power uniformity and the system efficiency (defined as the ratio of total power absorbed by the sample and the total power incident on the applicator).

3. MODELING OF THE EXPOSURE SYSTEM

The schematic diagram in Fig. 3 shows the exposure system main components : 1) the signal generator; 2) the microwave amplifier; 3) the bidirectional power sensor; 4) the coaxial cable; 5) the applicator. In the following the model of each of this subsystem is considered. The model of the overall system is obtained by assembling the models of the parts. For what concerns the signal generator, an ideal signal generator model is assumed, i.e. it is assumed that the system is able to produce, for the considered application, the desired electromagnetic field at a given frequency and with a prescribed constant power level.

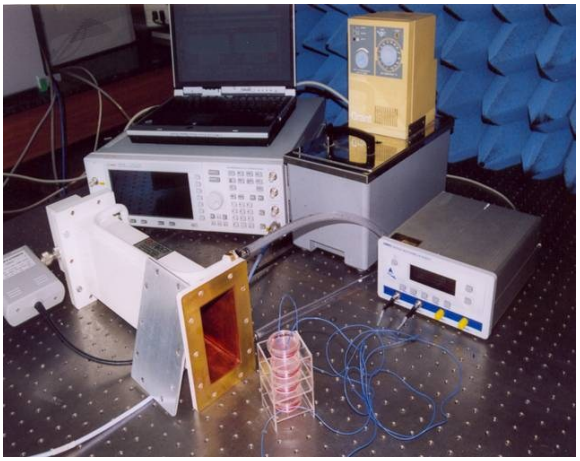

Fig. 1. The exposure system.

Fig. 2: The stand with four Petri cylindrical dishes.

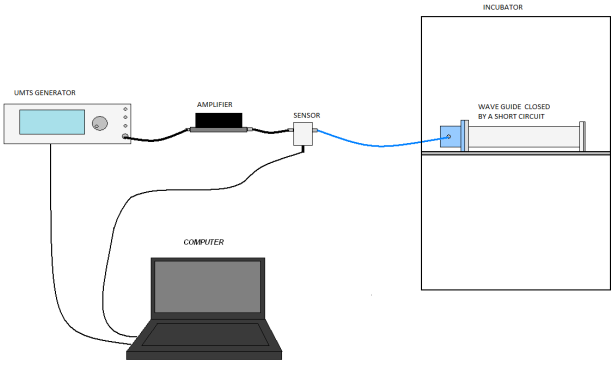

Fig. 3. Schematic of the experimental set-up for exposures and for local SAR measurements.

3.1 Microwave amplifier gain

The amplifier gain is defined as:

$$G = \frac{P_{load}}{P_{avail}} \qquad (1)$$

where P_{load} is the power delivered to the load by the amplifier, and P_{avail} is the power available from the source. The latter is the same as the power delivered to the amplifier input by the source (P_{gen}) under the condition that the amplifier input impedance is matched to the source impedance.

Assuming this was our case, that the system is linear and that small input signals will be used, then $P_{avail} = P_{gen}$ and G was evaluated by using the circuit sketched in Fig. 4: the source fed the amplifier and P_{load} was measured by the bidirectional power meter terminated with a matched load. By imposing at 1950 MHz a P_{gen} = 31.80 dBm (i.e., 0.66 μW), the obtained gain measurement is reported in Fig. 5. The average amplifier gain is 2.748×10^4, i.e. 44.39 dB , which is slightly less than the product specification (45dB).

3.2 Bidirectional power sensor

The transient response of the exposure system depends mainly on the dynamic response of the power meter used for the incident and reflected power measurements, and hence for SAR measurements. Some off-on and on-off tests were performed to identify the model structure and parameters, see Figs 6,7 where the measured SAR of the internal capsules is reported. Note that during the off phase an average bias of about 0.1 W/kg was detected. By performing experimental tests without the amplifier it is concluded that this bias is attributable to the specific sensor characteristic.

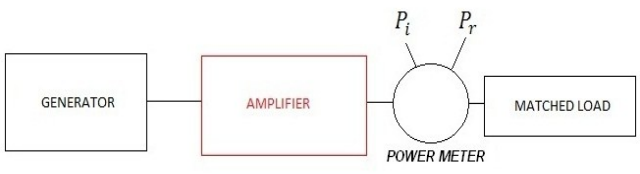

Fig. 4: A scheme for the amplifier gain computation, with $P_i = P_{load}$ and $P_r = 0$.

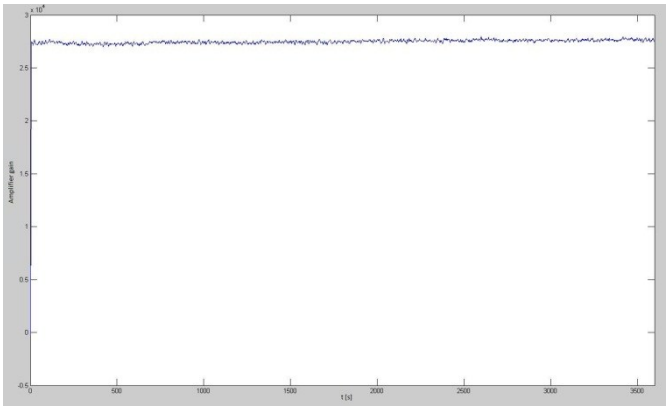

Fig. 5: The amplifier gain.

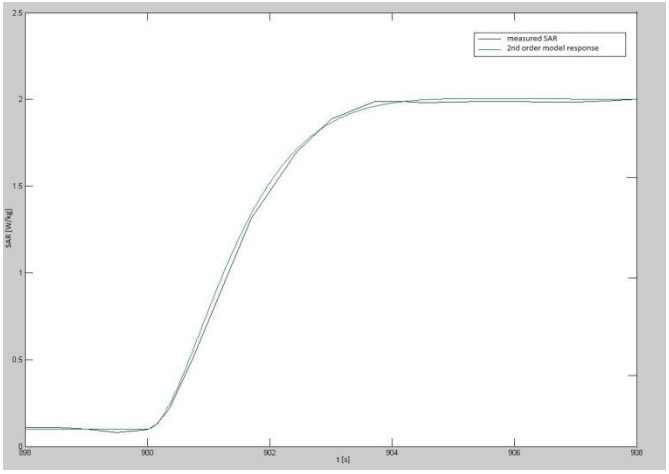

Fig. 6: Comparison between the measured SAR and the model output during the off-on test.

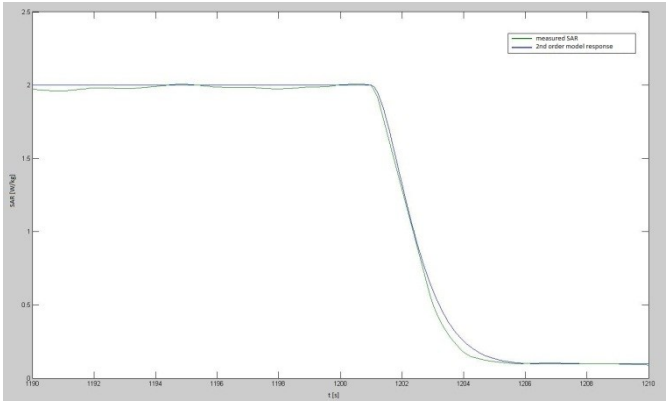

Fig. 7: Comparison between the measured SAR and the model output during the on-off test.

By eliminating the offset from the measurements, a second order LTI model provided the best trade-off between model accuracy and simplicity:

$$G(s) = \frac{\mu\omega_n^2}{s^2+2\xi\omega_n s+\omega_n^2}. \qquad (2)$$

From the experimental data the following parameters of the system are identified:

$$\mu \cong 1,\ \omega_n \cong 1.2,\ \xi \cong 0.9. \qquad (3)$$

3.3 Characterization of the coaxial cable

The coaxial cable can be modeled as a microwave two port reciprocal junction, characterized by a proper (symmetric) scattering matrix:

$$\bar{\bar{S}} = \begin{bmatrix} s_{11} & s_{21} \\ s_{21} & s_{22} \end{bmatrix} \quad (4)$$

For a generic scattering parameter the following definition can be used:

$$s_{ij} = \left. \frac{b_i}{a_j} \right|_{a_k=0 \ \forall k \neq j} \quad (5)$$

where a_j and b_i are respectively the incoming and outgoing signal. Each entry of the scattering matrix is frequency dependent. When $i \neq j$, then s_{ij} term is the transfer ratio from port *j* to port *i* (input *j*, output *i*), while the diagonal term s_{ii} represents the intrinsic reflection of the device at its port *i* when the other port is terminated on matched load, see Gardiol (1984).

The parameter needed for the cable characterization is the square modulus of the transmission coefficient that is defined as the ratio between the outgoing wave power and the incoming wave power, i.e.:

$$|s_{21}|^2 = \frac{P_{out}}{P_{in}} \quad (6)$$

By using a calibrated Vector Network Analyzer (VNA), with appropriate frequency settings, it is possible to measure the modulus and phase of the scattering parameters of the given coaxial cable for the UMTS frequency. In details, the coaxial cable scattering parameters were measured in the 1-3 GHz frequency range by means of a VNA Anritsu MS4623A, bandwidth 10 Mhz-6GHz.

The scheme of Fig. 8 was used where the coaxial cable to be characterized was inserted between two standard N-type cables. In Fig. 9 the measured $|s_{21}|$ in dB is reported.

At the 1.95GHz frequency the corresponding value is about -0,331 dB, or better, in a linear scale:

$$|s_{21}|^2_{f=1.95\ GHz} = 10^{\frac{-0.331}{10}} = 0.927 \ . \quad (7)$$

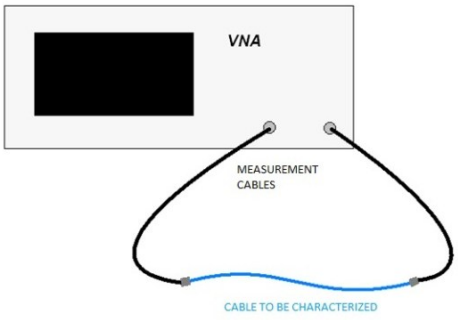

Fig. 8: The coaxial cable characterization.

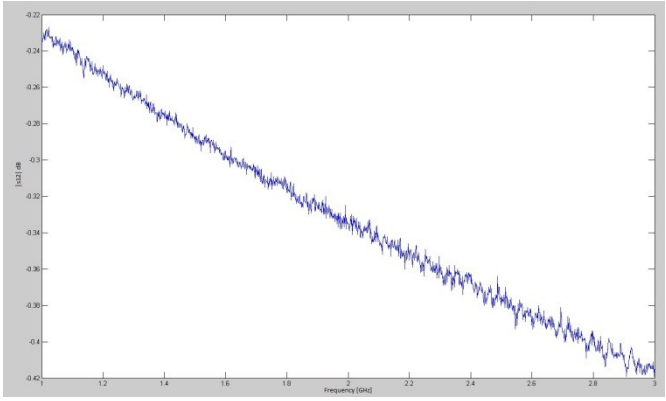

Fig. 9: The measured $|s_{21}|$.

3.4 Characterization of the applicator

It is possible to model the applicator by its static gain given by the sample efficiency *E*:

$$E = \frac{P_a}{P_i}, \quad (8)$$

where P_i is power at the input of the waveguide (at the output of the coaxial cable) and P_a is the absorbed power.

By neglecting the power losses due to the walls of the rectangular waveguide, the absorbed power of the dishes is assumed to be equal to the absorbed power measured at the power meter. Hence we can write:

$$P_a = SAR_i \cdot m_i + SAR_e \cdot m_e \quad (9)$$

where m_i is the total mass of the two internal dishes and m_e is the one of the external dishes. Assuming equal mass m for each Petri capsule, and knowing that the SAR relative to the internal capsules is 4 times higher than the SAR of the external capsules, it is:

$$P_a = \frac{5}{2} \cdot SAR_i \cdot m \ , \quad (10)$$

and hence:

$$SAR_i = \frac{2}{5} \cdot \frac{P_a}{m} = \frac{2}{5} \cdot \frac{(P_i - P_r)}{m} \ . \quad (11)$$

Assuming negligible power losses at the walls of the rectangular waveguide, it is also:

$$E = \frac{P_a}{P_i} = \frac{P_i - P_r}{P_i} = 1 - \frac{P_r}{P_i} \ . \quad (12)$$

From (11)-(12) it is clear that the evaluation of the incident power and of the reflected power allow the computation of both the capsules SAR and the applicator efficiency.

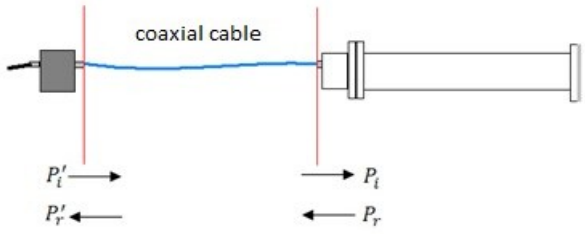

Fig. 10: The cable influence on the measured power.

Note that the power sensor measures the incident power $P_i^{'}$ and the reflected power $P_r^{'}$ at the input of the coaxial cable that propagates the field to the applicator. The P_i and P_r in (11),(12) are actually the incident and the reflected power at the input section of the waveguide, see Fig. 10.

The relationship between P_i, P_r and $P_i^{'}$, $P_r^{'}$ are the following:

$$P_i = P_i^{'} \cdot |s_{21}|^2 \,, \tag{13}$$

$$P_r = \frac{P_r^{'}}{|s_{21}|^2} \,, \tag{14}$$

where s_{21} is the coaxial cable transmission coefficient (see Sec. 3.3).

The numerical value of the applicator gain can be derived from laboratory measurements. By performing 3 different experiments with 4 on-cycles each (obviously in the off-cycles a null efficiency is obtained), the efficiency average value and variance can be determined for each on-cycle and for each experiment.

The obtained results are summarized by the following tables:

Table 1: Mean efficiency values.

	1st cycle [0,300] s	2nd cycle [900,1200] s	3rd cycle [1800,2100] s	4th cycle [2700,3000] s
E1	0.684	0.685	0.684	0.684
E2	0.684	0.684	0.685	0.684
E3	0.685	0.685	0.686	0.684

Table 2: Efficiency variance.

	1st cycle [0,300]s	2nd cycle [900,1200]s	3rd cycle [1800,2100]s	4th cycle [2700,3000]s
E1	2.762e-6	7.869e-6	3.951e-6	8.273e-6
E 2	2.561e-6	7.664 e-6	4.981e-6	9.070e-6
E3	2.302e-6	7.272 e-6	2.241e-4	6.132e-6

Since the variance is always extremely low, and the mean values are very similar, the experiment reproducibility is confirmed and the efficiency can be evaluated by computing the arithmetic mean of the mean values, i.e. a 0.685 value is adopted (about 70% efficiency).

3.5 The exposure system model

The overall system model was obtained by assembling the model of its components, according to the scheme of Fig. 3, and its validity was tested by several global tests. As an example, in Fig. 11 the simulated SAR of the internal dishes is reported for on-off cycles with 2 W/kg of maximum SAR. In Fig. 12 the corresponding experimental data show the good agreement with the simulation results.

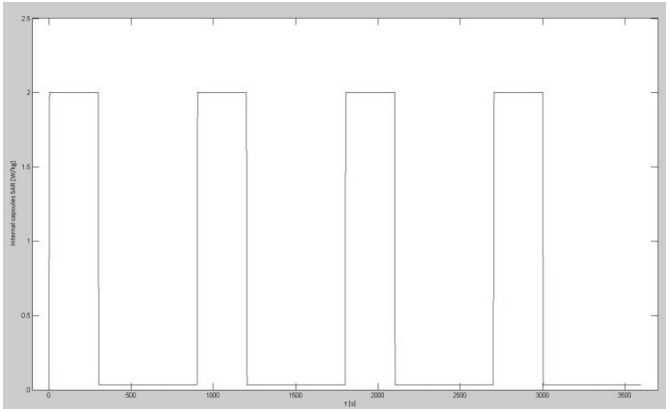

Fig. 11: Simulated SAR of the internal capsules.

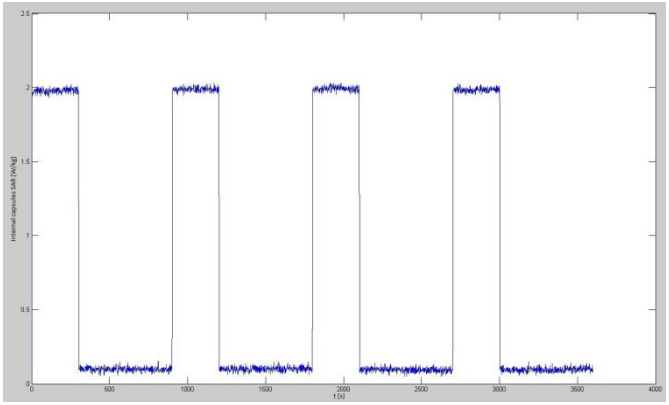

Fig. 12: Measured SAR of the internal capsules.

4. MODEL BASED PID DESIGN

The model of the exposure system can be used for the tuning of the PID controller parameters by employing the techniques available in the literature.

In the proposed control scheme the reference signal is assumed constant (or on-off) and corresponding to the desired SAR level. The current SAR is measured by the power sensor and used to evaluate the control error. The signal generator (the actuator) is accordingly commanded to produce the required incident power at the amplifier input.

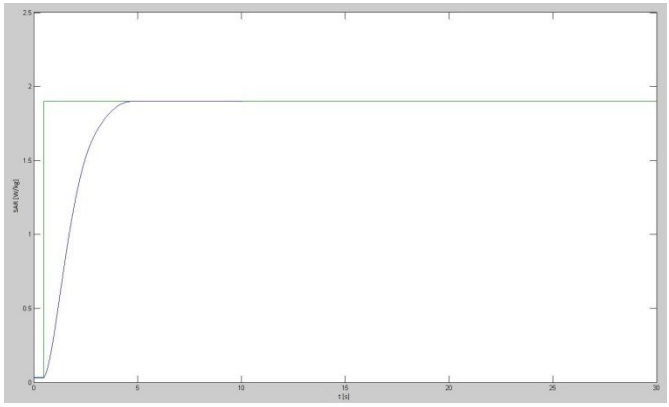

Fig. 13: Simulated controlled system step response.

The control objective is to regulate the amplitude of the generated field in order to maintain the measured SAR close to the desired SAR level, guaranteeing a less than 10s settling time and a less than 10% overshoot. For the settings of the PID control law a suitable Matlab/Simulink™ model of the exposure system has been developed. Taking into account the particular structure of the model, various open loop classical methods have been examined for the PID parameters tuning (see Åström and Hagglund (1995)).

In particular, the ITAE method provided satisfactory results, with a sufficiently low settlement time of about 4.68s and the absence of overshoot (see Fig. 13).

5. EXPERIMENTAL RESULTS

The proposed control scheme was verified by controlled exposure tests. The real-time implementation of the designed (equivalent discrete-time) PID controller was obtained through a specific LabView™ program. The management software implemented in LabView™ is characterised by an acquisition frequency of 10Hz, the maximal allowable for the power meter.

In Figs. 14,15 measured SAR variations are reported for off-on and on-off experiments respectively. The designed PID control still provides a sufficiently low settlement time and the absence of overshoot. Moreover, the standard deviation of the SAR level during the steady-state is limited.

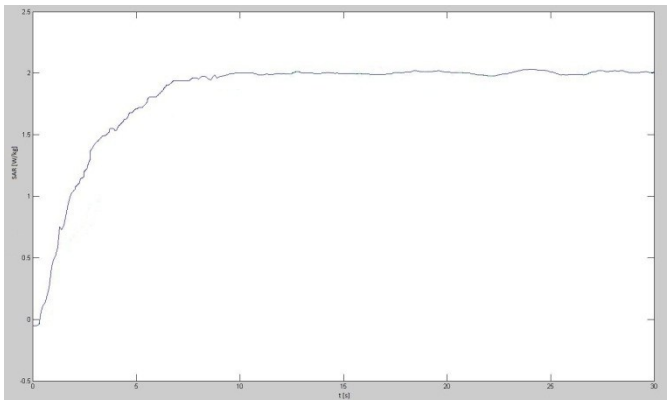

Fig. 14: Experimental off-on test for the controlled exposure system the designed PID action.

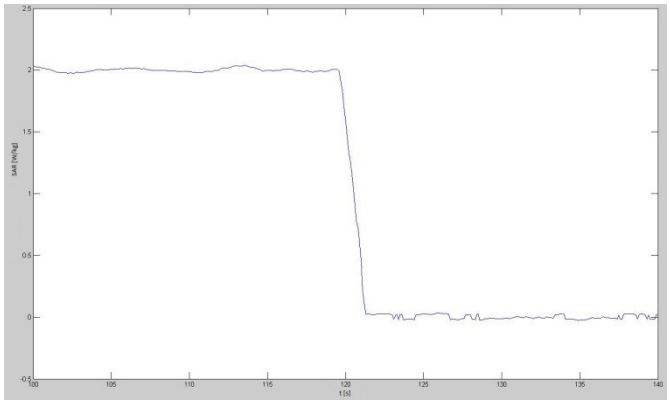

Fig. 15: Experimental on-off test for the controlled exposure system with the designed PID action.

6. CONCLUSIONS

The problem of the control synthesis for a microwave exposure system has been considered. After describing the system main components, a suitable control-oriented mathematical model has been derived by making use of experimental data. As a result, a model-based PID control has been designed by using classical PID tuning methods in order to satisfy the given requirements. The control system performance have been finally verified via closed-loop experimental tests.

REFERENCES

Åström, K.J., and Hagglund, T. (1995). *PID Controllers: Theory, Design and Tuning*. ISA, USA.

Calabrese, M.L., Castello, G., d'Ambrosio, G., Izzo, F., Grossi, G.F., Massa, R., Napolitano, M., Petraglia, G., Sannino, A., Sarti, M., Scampoli, P., Scarfì, M.R., Zeni, O. (2004). WITHER: Wireless Technology Health Risks, a Coordinated Bioelectromagnetic Research Project. In *Proceedings of Medicon and Health Telematics*, 221-224, Ischia, Italy.

Calabrese, M.L., d'Ambrosio, G., Massa, R., and Petraglia, G. (2006), A High-Efficiency Waveguide Applicator for *In Vitro* Exposure of Mammalian Cells at 1.95 GHz. *IEEE Transactions on Microwave Theory and Techniques*, 54 (5), 2256-2264.

Gardiol, F.E. (1984). *Introduction to Microwaves*. Artech House, USA.

Kuster, N., and Schönborn, F. (2000). Recommended minimal requirements and development guidelines for exposure setups of bio-experiments addressing the health risk concern of wireless communications. *Bioelectromagnetics*, 21, 508-514.

Moros E. G., and Pickard, W. F. (1999). On the Assumption of Negligible Heat Diffusion during the Thermal Measurement of a Nonuniform Specific Absorption Rate. *Radiation Research*, 152, 312-320.

Paffi, A., Apollonio, F., Lovisolo, G.A., Marino, C., Pinto, R., Repacholi, M., and Liberti, M. (2010). Considerations for Developing an RF Exposure System: A Review for in vitro Biological Experiments. *IEEE Transactions on Microwave Theory and Techniques*, 58 (10), 2702-2714.